PHASE TRANSFORMATIONS IN SINGLE CRYSTAL SI (110) INDUCED BY NANOINDENTATIONS AND HOLDING FORCE

Tei-Chen Chen and Yen-Hung Lin
Department of Mechanical Engineering, National Cheng Kung University, 701 Tainan, Taiwan

Introduction

Material of mono-crystalline Si has been extensively applied in a lot of fields in the past three decades. It has been verified by experiment that there exists Si-II (β-Sn, body-centred tetragonal structure) phase in high-pressure region on loading and amorphous-Si after unloading [1-2]. As the indentation loading is small and not yet induces plastic deformation, phase transformation of mono-crystalline Si still proceeds in an unstable manner. This unstable microstructure, however, will be partially recovered to the original one as the tip of indenter retracts from the specimen during unloading stage. In particular, the original mono-crystal Si may transform into metastable β-Sn when the loading is large enough to induce the onset of plastic deformation. Moreover, this microstructure may further permanently convert into amorphous phase during unloading stage [3, 4-5]. The amorphous phase is mainly composed of disarranged covalent bonds and fewer β-Sn. Moreover, it was already found that under higher unloading rate the material will transform from Si-II into Si-VII, Si-IX or amorphous phases [6-9]. As the pressure is released at a lower rate, Si-II undergoes a further phase transformation to the mixed phases of Si-III (BC8, body-centered-cubic structure) and Si-XII (R8, rhombohedral structure). Molecular dynamics simulations on structural phase transformations of mono-crystal Si during nanoindentation have been reported in recent publications [3, 10-14]. Some important results were reported in these studies. Although identification of structural phase transformations in the indented region was the main concern of these studies, the interpretation on the mechanisms of phase transformation for each phase, especially for crystalline BC8/R8, during cyclic loadings and unloadings was still insufficient. Therefore, the detailed mechanisms of cyclic nanoindentation-induced structural phase transformations and deformation behavior of mono-crystalline Si affected by the magnitude of loadings and surface orientations are investigated and discussed in this article by using MD simulations. A large cell containing more than half million Si atoms is adopted to facilitate the observation of phase change. Moreover, the effects of holding force on the structural phase transformation of mono-crystalline Si on (110) surface are also evaluated and discussed.

Molecular Dynamics Simulations

The inter-atomic potential function proposed by Tersoff [15] that considered the effect of bond angle and covalent bonds has been shown to be particularly feasible in dealing with IV elements and those with a diamond lattice structure such as C, Si, and Ge. The Tersoff function [29] is therefore adopted in this study to analyze the dynamic correlations in C-C and Si-Si atoms. In regard to the mutual interaction between C and Si under the equivalent potential, we use the two-body Morse potential, which has been well described for C-Si atoms. Although a two-body potential leads to less precise solutions than a many-body potential does, it is still satisfactorily employed in MD simulations through the accurate calibration of parameters by spectrum data. The choice of these potentials is supported by the previous simulations and tests, which showed good an agreement between simulation results and experimental data [16-17]. The periodic boundary conditions are imposed on the four side surfaces of the substrate. The two layers on the bottom of the substrate are fixed to provide structural stability and to avoid large reactions and rebound forces. The four layers above the fixed layers are set as free motion layers while the remaining layers are thermal control layers that stabilize the temperature of the physical system. In this work, the time step is as short as 1 fs to ensure solution accuracy. A modified five-step methodology is used to incorporate Newton's equations of motion so that the position and velocity of a particle can be effectively evaluated. Moreover, the mixed neighbor list is applied to enhance computational efficiency.

Results and discussion

The original phase prior to loading is Si-I, while the other four phases created during loading and after unloading are, respectively, high-pressure phase with coordination number more than 6 colored by red, Si-II phase colored by yellow, BCT5 phase denoted by blue, and mixed phases of BC8 and R8 colored by green. Figures 1 and 3 show the side cross-sectional views of the transformation zone and shape of residual indent on (110) Si after the first and fifth indentation cycles, respectively, when subjected to two different magnitudes of P_{max} = 8000 and 12000 nN, respectively. It is seen that, at the end of the first indentation cycle, the residual Si-II, mainly induced by plastic deformation, is almost absent under the load of P_{max} = 8000 nN. Only a limited number of BC8/R8 appears as the residual phases distributed within a small region. On the other hand, it can be seen that a very significant plastic deformation and residual indent can be observed for the larger load P_{max} = 12000 nN. After finishing five indentation cycles, compared to the situation at the

end of the first indentation cycle, both the size of the transformation zone and residual indent are significantly increased for P_{max} = 8000 nN, while there is no significant change for P_{max} = 12000 nN. Moreover, it is seen that a significant part of transformed phases that are distributed over the region of elastic deformation on loading will be recovered to the original mono-crystal Si-I structure as the loading is released.

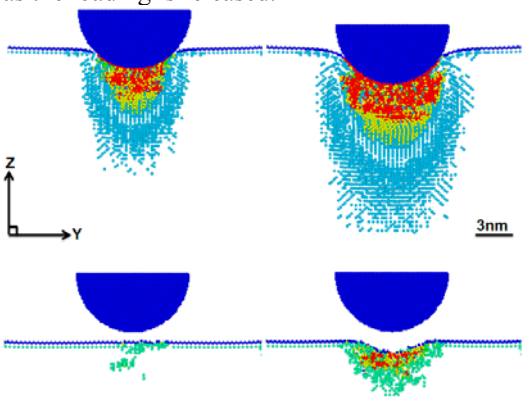

(a) (b)

Fig. 1 Side cross-sectional views of the transformation zone and shape of residual indent on (110) Si under the maximum loading (a) P_{max} = 8000 nN and (b) P_{max} = 12000 nN after the first indentation cycle.

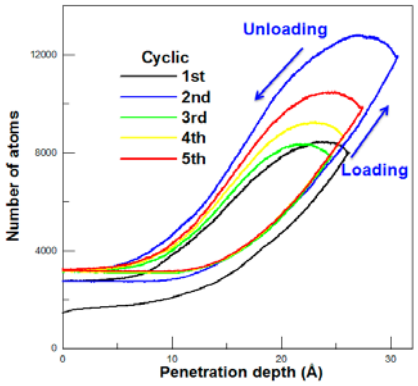

(a)

Fig. 2 Variation of total number of transformed atoms in each cyclic indentation cycle on (110) Si at P_{max} = 8000 nN

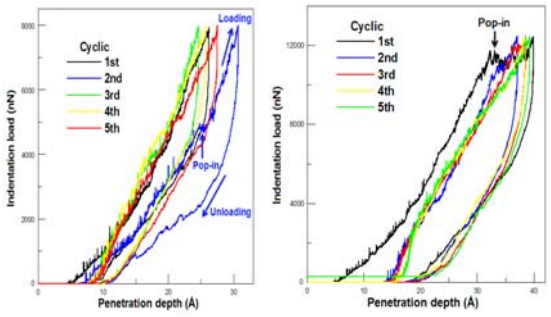

(a) (b)

Fig. 3 Load-displacement curves for each indentation cycle on (110) Si at (a) P_{max} = 8000 nN and (b) P_{max} = 12000 nN

Conclusion

The structural phase transformations induced by five repeated indentation cycles under the same maximum loading on (110) oriented mono-crystalline Si surfaces are examined by MD simulations. It can be observed that the amounts of transformed phases all tend to increase after repeated indentations under different maximum loadings. As the maximum loading in the first indentation cycle is too small to induce phenomenon of pop-in, a softer hardness is exhibited in the transformation zone. Consequently, a much deeper indentation depth, associated with a significant increase in the amounts of transformed phases of Si-II, high-pressure, and BC8/R8, might be formed during the subsequent indentation cycles. After finishing this critical indentation cycle, both the maximum indentation depth and the number of each transformed atoms almost remain unchanged. On the other hand, as the loading in the first indentation cycle is large enough to induce large plastic deformation region, a greater hardness is exhibited in the transformation zone due to formation of high-pressure mixed in the amorphous. Consequently, a much smaller indentation depth, associated with a slow increase in the transformed atoms of Si-II, high-pressure, and BC8/R8, will be formed during the subsequent indentation cycles.

Acknowledgement

This research was supported in part by the National Science Council in Taiwan through Grants Nos. NSC 95-2221-E-006-273, NSC 96-2221-E-006-051 and NSC97-2917-I-006-113.

References

1. Callahan, D. L. and Morris, J. C., *J. Mater. Res.* **7** (1992) 1614.
2. Domnich, V. and Gogotsi, Y., *Appl. Phys. Lett.***76** (2000) 16.
3. Cheong, W. C. D. and Zhang, L. C., *Nanotechnology* **11** (2000) 173.
4. Zhang, L. C. and Tanaka, H., *JSME Inter. J.* **A42** (1999) 546.
5. Cheong, W. C. D. and Zhang, L. C., *J. Mater Sci Lett.***19** (2000) 439.
6. Crain, J., Clark, S. J., Ackland, G. J., Payne, M. C., Milman, V., Hatton, P. D. and Reid, B. J., *Phys. Rev. B* **49** (1994) 5329.
7. Crain, J., Ackland, G. J., Maclean, J. R., Piltz, R. O., Hatton, P. D. and Pawley, G. S., *Phys. Rev. B* **50** (1994) 13043.
8. Piltz, R. O., Maclean, J. R., Clark, S. J., Ackland, G. J., Hatton, P. D. and Crain, J., *Phys. Rev. B* **52** (1995) 4072.
9. Kim, D. E. and Oh, S. I., *Nanotechnology* **17** (2006) 2259.
10. Lin, Y. H. and Chen, T. C., *Applied Phys. A* **92** (2008) 571.
11. Lin, Y. H., Jian, S. R., Lai, Y. S. andYang, P. F., *Nanoscale Res. Lett.* **3** (2008) 71.
12. Cheong, W. C. D. And Zhang, L. C., *J. Mater. Sci. Lett.* **19** (2000) 439.
13. Zarudi, I., Zhang, L. C. and Swain, M. V., *Appl. Phy. Lett.* **82** (2003) 1027.
14. Zarudi, I., Zhang, L. C., and Swain, M. V., *J. Mater. Res.* **18** (2003) 758.
15. Tersoff, J., *Phys. Rev. Lett.* **56** (1986) 632.
16. Zhang, L. C. and Tanaka, H., *Wear* **211** (1997) 44.
17. Zhang, L. C. and Tanaka, H., *Tribol. Int.* **31** (1998) 425.